SLAC-PUB-11886
May 2006

EMC DIAGNOSIS AND CORRECTIVE ACTIONS FOR SILICON STRIP TRACKER DETECTORS

F. Arteche[(1) (2)] and C. Rivetta[(3)]
[(1)] CMS Central Tracker (CMT), PH Department, CERN
CERN,1211 Geneve 23 Switzerland
E-mail: fernando.gonzalez.arteche@cern.ch
[(2)] High Energy Physics group, Imperial College, University of London
[(3)] Accelerator Technology Research Department, Stanford Linear Accelerator Center (SLAC)
Stanford, CA 94305 U.S.A
E-mail: rivetta@slac.stanford.edu

Abstract: The tracker sub-system is one of the five sub-detectors of the Compact Muon Solenoid (CMS) experiment under construction at CERN for the Large Hadron Collider (LHC) accelerator. The tracker sub-detector is designed to reconstruct tracks of charged sub-atomic particles generated after collisions. The tracker system processes analogue signals from 10 million channels distributed across 14000 silicon micro-strip detectors. It is designed to process signals of a few nA and digitise them at 40 MHz. The overall sub-detector is embedded in a high particle radiation environment and a magnetic field of 4 Tesla.
The evaluation of the electromagnetic immunity of the system is very important to optimise the performance of the tracker sub-detector and the whole CMS experiment. This paper presents the EMC diagnosis of the CMS silicon tracker sub-detector. Immunity tests were performed using the final prototype of the Silicon Tracker End-Caps (TEC) system to estimate the sensitivity of the system to conducted noise, evaluate the weakest areas of the system and take corrective actions before the integration of the overall detector. This paper shows the results of one of those tests, that is the measurement and analysis of the immunity to CM external conducted noise perturbations.

I. INTRODUCTION

The CMS detector is one of the high-energy physic experiments of the Large Hadron Collider (LHC), under construction at CERN, Switzerland. The CMS detector is composed by different sub-detectors whose mission is identify the track and the energy of sub-atomic particles after hadron collisions. One of those sub-detectors is the *Silicon Tracker*; it is located in the interaction region of the calorimeter and its function is to measure the track of particles after collision. The tracker sub-detector has two parts; the inner one based on *Pixel detectors* and the outer part built with *Silicon micro-strip detectors*. Figure 1 depicts the mechanical layout of the tracker sub-detector. This sub-detector operates under high particle radiation, a temperature around -20 degrees Celsius and is immersed into a DC magnetic field of 4 Tesla.

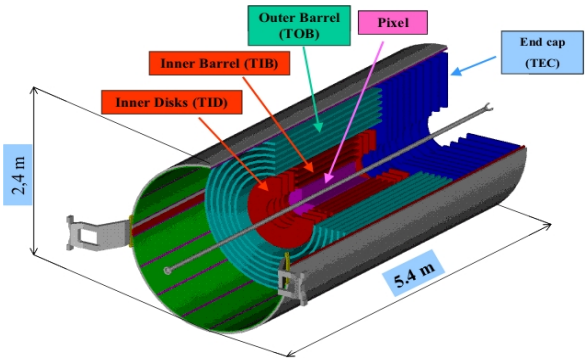

Fig. 1. Mechanical layout of the silicon micro-strip and pixel tracker sub-detector.

The detector module is the basic functional component of the silicon tracking system. Each module consists of three main elements:

- Single or double side silicon micro-strip sensors.
- Mechanical support (Carbon fibre frame).
- Readout front-end electronics (Hybrid circuit).

A general layout of the module, showing the three main elements is depicted in Fig. 2. These modules are grouped, partially overlapped, in leaders and petals to cover several cylinders and end-caps of the mechanical structure showed in Fig. 1.

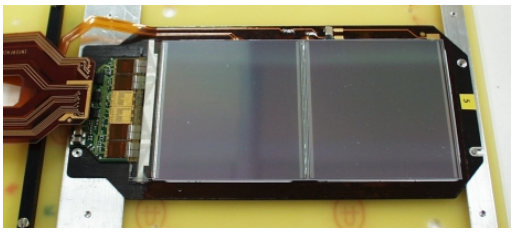

Fig. 2. Tracker module layout

The silicon tracker readout electronics [1] processes analogue signals from 10 million channels distributed across the silicon micro-strip detectors. It has four different parts;

- The micro-strip detector or sensor.
- The charge amplifier – APV25.

7 th EMC Europe International Symposium on Presented at Electromagnetic Compatibility, 4-8 September, 2006, Barcelona, Spain

Work supported in part by Department of Energy contract DE-AC02-76SF00515

- The control unit, located in the detector.
- The front-end controller and front-end driver located in the counting room, 100 meters away from the detector.

Each micro-strip of the detector is read-out by a charge sensitive amplifier (APV25)[1] whose output voltage is sampled at 40 Msamples/sec. Samples are stored in an analogue pipeline for a few milliseconds and following a trigger signal, they are processed by an analogue circuit using a weighted sum algorithm to measure the signal amplitude and the associated bunch crossing to the hit. Processed data from different APV25 chips is multiplexed in time and sent over a short twisted pair cable to a laser diode, where electrical signals are converted to infrared light and transmitted over 100 meters through optical fibre to the counting room, adjacent to the detector cavern.

The most sensitive component of the silicon tracker readout electronics is the charge amplifier. The APV25 is a 128-channel analogue pipelined custom chip used to read-out the silicon micro-strip detectors. The chip is fabricated in a standard 0.25-µm CMOS process to take advantage of the radiation tolerance, high-density integration, low noise and low power consumption. Each channel is composed by a low noise amplifier, a 192-cell analogue pipeline and a de-convolution filter. The APV25 has two different operation modes, the peak mode (PEAK) and the de-convolution mode (DEC), with different bandwidths.

The total number of silicon tracker detector modules is 13884 and the number of APV25's reading those detectors is around 80000. Groups of 6 and 12 detector modules are powered from a single power supply unit. The silicon tracker needs around 250 kW of power to operate. About 2000 power supply (PS) units are required for the silicon tracker detector. Each PS unit supplies three different voltages to a specific group of modules. Two low voltages, 2.5V and 1.25V, with a common power return are used to supply the front-end electronics (FEE), while a 500V PS is used to bias the micro-strip sensors. Power supplies are located on the periphery of the CMS detector, 40 meters away from the tracker sub-detector.

In the design of the FEE for the tracker sub-detector, the noise perturbing the signal detected should be sufficiently low to ensure high efficiency and bunch crossing identification. This paper addresses the EMC studies focused on the quantification of the FEE sensitivity to conductive noise coupled through the input/output cables, focusing in the common mode immunity of the system. This analysis is part of the EMC plan [2] focused to control the electromagnetic (EM) emissions and immunities of the sub-systems to ensure the correct integration of the CMS experiment.

II. EMI CHARACTERIZATION OF TRACKER

Since the tracker FEE is linked to the acquisition system via optical fibres, the conductive noise is mainly coupled into the FEE through the input power cables and the slow control network. EMC of the overall FEE can be achieved imposing EMC-based design to the system. The EMC can be either evaluated at early stage of the system design via modelling and simulation [3] or measured on prototypes [4]. In the first case, the design can be conducted imposing EMC constraints, whereas in the second case, it is possible to identify from the prototype critical elements and inappropriate layouts that are responsible for the performance degradation of the FEE. To characterize the electromagnetic susceptibility of the FEE to conductive disturbances, different tests are conducted by injecting RF currents through the FEE input power and slow control cables. These tests have two goals: first, the tests will characterize the immunity of the system to RF perturbations defining weak points in the design, which allows taking corrective actions before final production. Secondly, the noise characterization will provide data to define the emission level to be imposed to the equipment connected to the front-end electronics. These tests allow quantifying the FEE sensitivity to conductive noise to define the output noise level of power supplies, the magnitude of both external EM fields and ground currents, etc.

II.1 Test Set-up

The experimental set-up is designed such that the FEE and the auxiliary equipment exhibit during the test a configuration as close as possible to the final one. The FEE and the auxiliary equipment are placed on a copper plane as suggested by IEC-61000 [5]. This copper sheet is the reference ground plane. The perturbing signal is injected to the FEE input power and slow control cables using a bulk injection current probe, a RF amplifier and a RF signal generator. The use of the bulk current injection (BCI) technique to study the noise effects induced by EM radiation on a system is well known in aerospace, military and automotive industry. Several papers [6] [7] have shown the advantages, disadvantages and complexity of this technique to achieve good results. The level of the injected signal is monitored using an inductive current clamp and a spectrum analyser. To represent the effect of very long cables, normalized common impedances (CI) based on lumped components are inserted between the power supplies and the FEE to standardize the measurements. The test procedure consists of injecting a sine-wave perturbing current at different frequencies and amplitudes into the FEE through the input cables and evaluating the performance of the FEE, measuring the output noise signal. The output signal of the FEE is measured by its own acquisition system. The frequency range of the injected RF signal is between 150 kHz and 50 MHz.

The results presented in this paper correspond to EMC tests conducted on a FEE prototype of one of the CMS tracker sub-systems, the Tracker End-Caps (TEC) [8].

The prototype used to perform the EMC tests consisted of a *'petal'* with 96 APV25 chips and associated electronics distributed along one interconnection board (ICB). The individual modules connected to the ICB in the prototype are shown in Fig. 3. The complete experimental set-up to study the RF immunity of the FEE is shown in Fig. 4, where the rectangular box holds the petal depicted in Fig. 3. Further information about the TEC FEE can be found in [8].

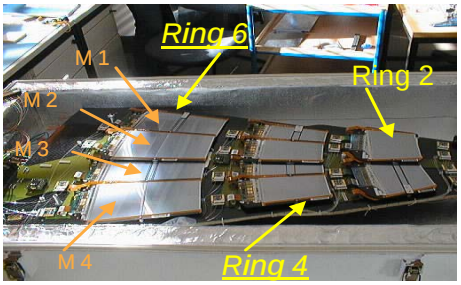

Fig. 3. Petal corresponding to the TEC prototype tested. It shows Rings 2, 4, 6 and the location of the modules.

For this sub-detector, the noise requirements sets the overall thermal noise contribution of the APV25 amplifier to the system to a maximum of 2 counts RMS at the output of the ADC. It is equal to a noise of 1.64mVRMS (1.22counts/1mV) at the input of the ADC or an equivalent RMS charge noise at the input of the APV25 of 40 fC (2500 electrons). The prototype tested includes about 12500 channels and the output noise level spans between 0.8 and 2 counts RMS when no RF perturbation is injected.

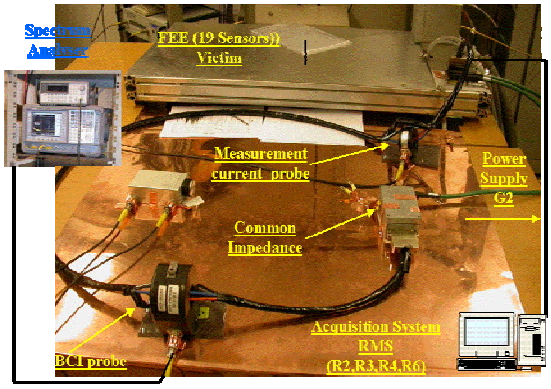

Fig. 4. Test layout.

III.2 EMI characterization to CM currents in power cables.

To study the effect of common mode (CM) noise currents flowing through the internal power conductors, the BCI method is applied, injecting the perturbation current to both the active and return power cables. In practice, this CM noise is generated by power supplies and coupled to the FEE through long cables. The procedure to conduct this test is similar to the one previously analysed for HCAL detector [4]. A sine-wave current is injected through the power cables as CM perturbation and the FEE output signal is measured by its acquisition system. The sine wave injected will perturb the FEE by adding a noise component to the intrinsic thermal noise component of the APV25. The level of the signal injected is large enough to have a good signal-to-noise ratio at the input of the ADC without affecting the linearity of the overall FEE.

The injected currents to the FEE affect its performance and the interference depends on the amount of noise current coupled to the sensitive areas of the FEE. Due to slight differences in the connection between the modules and the ICB, the perturbing current does not affect all modules equally. Modules located in Rings 4 and 6, near the central part of the petal (Module 3 is the closest to the ICB board), are the most sensitive. Additionally, due to the particular connection between APV25 chips to the micro-strip detector, the noise does not distribute equally across all channels.

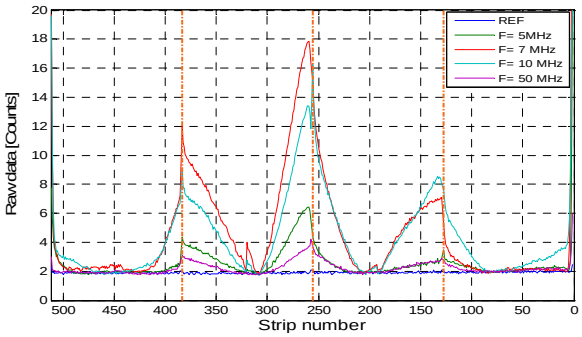

Fig. 5. Noise distribution per channel in Module 3 of Ring 6 at 5MHz, 7MHz, 10 MHz and 50 MHz.

Partial results of the conducted noise tests performed are summarized in Fig. 5. This figure shows the variation of the RMS value of the digitised voltage at the output of the tracker FEE for all the channels in four different APV25 of the same module (Module 3) located in ring 6, when the perturbing currents are sine waves whose level is 92 mA RMS and their frequencies are 5, 7, 10 and 50 MHz. The RMS output voltage includes both the intrinsic thermal noise of the APV25 and the noise due to the injected current. It can be observed that the noise does not distribute equally for all the channels of the same micro-strip detector. APV25 channels located close to the edge of the chip represent the worst case and the one located in the centre of the chip are practically insensitive to the injected noise. This coupling mechanism for the noise in the tracker system will be explained in detail in section II.2.1

The FEE immunity to CM currents can be quantified by the function defined as the ratio between the AC component of the output voltage, due to the injected CM current, and the injected current. Mathematically, it can be expressed as:

$$TF(\omega) = \frac{V_{1out}(\omega)}{I_{1cm}(\omega)} \quad (1)$$

where, $I_{1cm}(\omega)$ is the magnitude of the perturbing sine wave signal and $V_{1out}(\omega)$ is the magnitude of the AC output voltage. Based on the test results, it is possible to characterize the susceptibility of each channel of the FEE. The output voltage magnitude $V_{1out}(\omega)$, which corresponds to the FEE response to the injected current, is calculated from the RMS digitised output voltage and (1) is evaluated for each channel recorded.

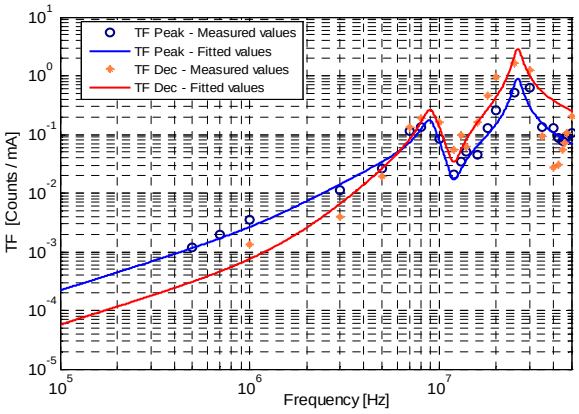

Fig. 6. Measured average sensitivity function to CM currents for the APV25 number 2 - Ring 6 - Module 3.

Figure 6 shows the function $TF(\omega)$ for some of more noisy channel of the prototype. It corresponds to data evaluated between 100KHz and 50MHz with the APV25 operating in both PEAK mode and DEC mode. The measured values can be fitted to a mathematical model that represents the FEE sensitivity to CM currents in the frequency range depicted in Fig. 6. This figure shows a few important things:

- PEAK mode is more sensitive than DEC mode at low frequency, but at high frequency the DEC mode is more sensitive.
- There are two resonances, which are associated to the ICB and ground connections.

This analysis allows us quantifying the sensibility of the FEE to CM noise currents. It is used to understand the coupling mechanism between the external noise currents and the sensitive parts of the FEE and apply corrective actions in case of being necessary. Additionally, the CM sensitivity of the FEE can be used to define the level of the external CM noise contribution that the FEE can tolerate without affecting its performance. For example, to define the specific CM emission levels compatible with this FEE of the power supply units.

II.2.1 Coupling Mechanism – EMC diagnosis

The identification of the coupling mechanism of external noise current into the sensitive FEE is of prime importance to take corrective actions to improve the immunity of the FEE. Assuming the noise is coupled through the input of the APV25 in the frequency range analysed, the function $TF(\omega)$ measured before can be decomposed in two terms. One corresponds to the transfer function of the APV25 channels and the other defines the ratio between the perturbing current injected and the current that flows through the APV25 input signal circuit. The second term gives the necessary information to identify the coupling mechanism of the noise in the system. Therefore, the function $TF(\omega)$ is

$$TF(\omega) = \frac{I_{APV}(\omega)}{I_{1cm}(\omega)} \cdot \frac{V_{1out}(\omega)}{I_{APV}(\omega)} = H_{apv}(\omega) \cdot H_c(\omega) \quad (2)$$

The APV25 transference function $H_{APV}(\omega)$ has been characterized quantifying the impulse response of the device. Based on this information, the transfer function $H_C(\omega)$ in (2) can be estimated based on our measurements. Figure 7 shows the function $H_C(\omega)$ based on the $TF(\omega)$ function previously measured in the frequency range between 100 KHz and 50 MHz for the APV25-2 located in the Ring 6 - Module 3. The function $H_C(\omega)$ is fitted by a function that models the transfer function of the coupling network between the injected current $I_{1cm}(\omega)$ and the APV25 input current $I_{APV}(\omega)$.

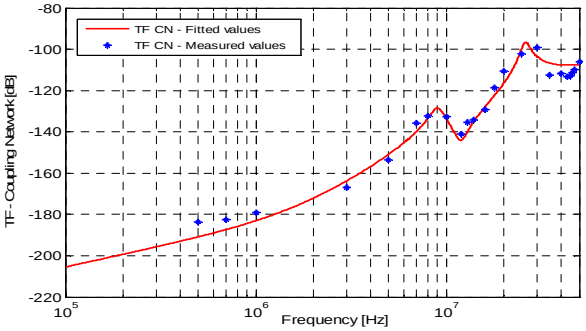

Fig. 7. Transfer function of the coupling network calculated from previous measurement for the APV25 number 2 - Ring 6 - Module 3.

The coupling network $H_C(\omega)$ is characterized by 3 dominant terms :

- At low frequency, the function increases 20 dB per decade
- The first resonance frequency is at 8.5MHz
- The second resonance frequency is at 28.5MHz.

The assumption that the injected noise is mainly coupled into the input of the APV25 amplifier implies that it is necessary to analyse the signal circuit defined by the APV25 and the micro-strip detector to understand the coupling mechanism. A simplified electric scheme is shown in Fig. 8. One of the 512 diodes that compose the micro-strip detector is depicted in this figure. Micro-strips detectors are biased using a 500V power supply and resistors of 2 Mohms. In normal operation, when a sub-atomic

particle hits a micro-strip, they induce in the diode an impulse current signal, which is AC coupled to one of the 128 channels of the APV25. This signal flows through the loop defined by the diode itself and its parasitic capacitance *Cd*, the parasitic capacitance between the detector and the carbon fibre, *Cmec*, the carbon fibre frame, the parasitic capacitance between this frame and the hybrid ground plane, the by-pass capacitor, the input impedance of the APV25 and the coupling capacitor *Cc*. This loop is indicated in Fig. 8.
The 128 channels of the APV25 have independent inputs, being the reference of each amplifier common for all of them. The references are all connected inside the chip to the same distribution-bar, which is referred to the 1.25V line. This particular design constraint is because it is necessary to achieve reduced power consumption in the chip. The 1.25V distribution-bar is AC coupled to hybrid ground via a single capacitor connected to a pin located in the central part of the chip (It is physically located in the middle of the 128 channels). The 1.25V distribution-bus is part of the input signal loop for all the APV25 channels. Any noise current flowing through the distribution-bus produces a distributed voltage drop that affects the individual input current I_{APV} per channel. Its effect is more severe for those channels distant from the central point of the chip.

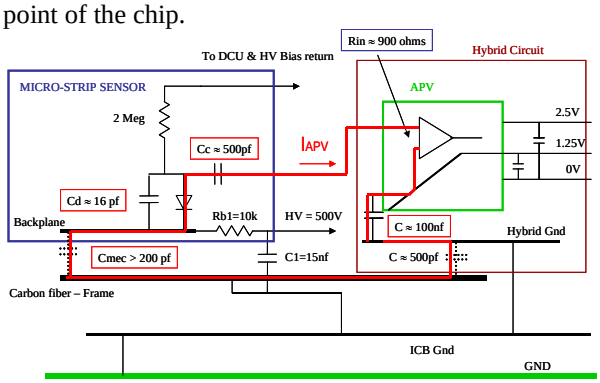

Fig. 8. Detector – APV25 signal circuit.

For the CM test, currents are injected externally to the prototype through a bundle of power conductors created by the 2.5V, 1.25V and 0V lines, being the return for the injected current the ground circuit. The prototype tested does not include CM filters, being the only filter for the power supply lines capacitors distributed across the ICB and the hybrid boards connected between 2.5V and 0V lines and 1.25V and 0V lines (differential mode filters).
In the prototype, the injected current flows through the 2.5V, 1.25V and 0V lines in the ICB and part of it flows through the power lines of each hybrid board. This fraction of current flowing through the hybrid is in inverse proportion to the impedance of the connection between the hybrids and the ICB. Larger fraction of current flows through those hybrid circuits located above the ICB, being the hybrids located away of the distribution line of the ICB less affected. At the hybrid level, in particular in each APV25 chip, a fraction of the current flows through the 1.25V distribution-bus inside the chip toward the connection between this line and the hybrid ground defined by the by-pass capacitor of 100nF (Fig. 8.). This connection divides the distribution-bus in two halves; with 64 APV channels connected at each half. The CM current finds its return through both the connections between the hybrid ground and the carbon fibre frame with the ICB ground.
Noise currents flowing through the 1.25V distribution-bus induce a distributed voltage proportional to the partial inductance of the bus. It is well known [9][10] that rectangular conductor inside chips present inductances of the order of *pHy-nHy*. This voltage drop appears as a voltage generator in series in the input signal loop of each channel of the APV25, being the noise contribution larger for those channels located far away of the 1.25V distribution-bus connection to ground at the central part of the chip (Effect depicted in Fig. 6).
The distributed noise voltage induced by the CM current is defined by $V_N(\omega,x) = j\,\omega\,L_{APV}(x)\,I_P(\omega)$, where; $I_P(\omega)$ is the current flowing through the 1.25V distribution-bus, $L_{APV}(x)$ the partial inductance of the bus, x the distance along the bus from the central point and $V_N(\omega,x)$ is the distributed voltage drop across the 1.25V bus. This voltage forces a noise current at the input of each APV25 channel limited by the impedance of the input signal loop. From Fig. 8, this impedance can be approximated in a frequency range up to 10MHz as $Zl = Rin + 1/j\omega Ceq$, being *Rin*, the input impedance of the APV25 (Rin = 900ohms) and *Ceq*, the total magnitude of all the capacitors in the input loop connected in series. Then, the input current is

$$I_{APV}(\omega,n) \cong \frac{I_p(\omega)\, j\,\omega\, L_{APV}(x)}{Rin} \qquad (3)$$

At low frequency, the current $I_P(\omega)$ is related to the injected current $I_{1cm}(\omega)$ by a proportional factor depending upon the relative impedance among power distribution lines of each hybrid respect to the ICB. Defining this proportional factor per APV25 chip as α_{APVi}, then $I_P(\omega) = \alpha_{APVi}\, I_{1cm}(\omega)$. Finally, at low frequency, the transference function defining the coupling mechanism of the CM currents into the APV25 can be expressed as:

$$\frac{I_{APV}}{I_{cm}} \cong \alpha_{APV_i} \cdot \frac{j\,\omega\, L_{APV}(x)}{Rin} \qquad (4)$$

The constant α_{APVi} defines the noise distribution per ring and module. This value is always lower than one and depends of the position of the module per ring and per ICB.
The CM current, after flowing through the hybrid board, returns to ground via the hybrid board and ICB grounds and their connections to ground. This return circuit have parasitic capacitances associated with the carbon fibre structure and the ICB. Those stray elements resonate with the inductance associated with

the ground connections defining the two resonances depicted in previous figures. To identify those resonances in the prototype, new measurements were performed. It showed that the 8.5MHz resonance corresponds to the resonance between the ICB and reference plane and the 28.5MHz resonance corresponds to the carbon fibre and the ICB. A more details analysis of this resonance in the structure is planned in the near future.

II.2.2 Corrective actions – EMI Filter

The coupling mechanism depends of three factors:

- APV inductance
- Resonance of the circuit
- Amount of current flowing in the 1.25V line.

The CM immunity of TEC front-end electronics can be improved if the APV inductance is minimized, the circuit resonances are controlled and the amount of noise current flowing through the input loop of the APV is reduced.

The first possible solution requires a redesign of the APV25 chip internal layout and is impossible at this stage of the project. The 8.5MHz resonance associated with the ICB ground connection will be improved in the final installation building a 3-D grid structure to ground the ICB via multiple short traps.

To limit the noise current flowing through the 1.25V distribution-bus inside the APV25, a CM filter can be installed either at the input power of each Tracker petal or at the input power of each APV25 chip. The last option represents a problem due to the large amount of elements to be included in the Tracker system, reducing the overall reliability. Locating a CM filter at the input power terminals per petal reduce the amount of filters and avoids the EM radiation of the power inside the faraday cage where the tracker is located. A limiting constraint for this CM filter is that it must be implemented without any magnetic component. To quantify the improvement with this filter, a new CM test was performed including the CM filter implemented with 3 capacitors of 1µF. Results depicted in Fig. 9 shows a general improvement between 12-30 dB, taking as reference the same APV25–2, Ring 6–Module 3, operating in PEAK mode.

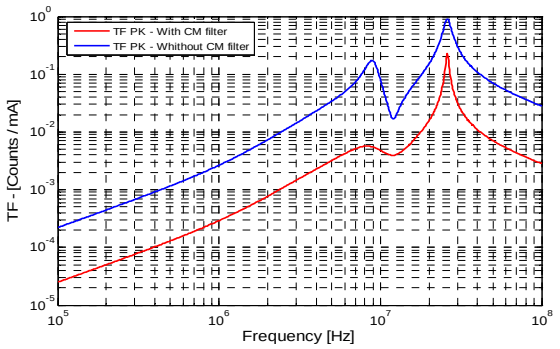

Fig. 9. Comparison of the sensitivity functions to CM currents with and without CM filter.

IV. CONCLUSION

Immunity tests for conductive noise have been conducted on a prototype of the TEC sub-detector. The tests quantify the susceptibility of the FEE and also allow identifying the coupling mechanism between the injected noise and the sensitive areas of the system. This information is used to define solutions to improve the EM immunity of the system before final integration. Proposed solutions find some limitations that need to be evaluated in a frame of technical, risk and economic issues.

REFERENCES

[1] M. Raymond, *et. al., "The APV25 0.25 µm CMOS readout chip for the CMS Tracker"*, Proc. IEEE Nuclear Science Conference, October 2000, Lyon, France, pp. 9/113 - 9/118,.

[2] F. Arteche, *et.al. "Electromagnetic compatibility plan for the CMS detector at CERN"*, Proc. of 15th Int. Zurich Symposium on EMC, February 2003, Zurich, Switzerland, pp. 533-538.

[3] F. Arteche and C. Rivetta, *"Noise Susceptibility Analysis of the HF Front-End Electronics for the CMS High -Energy Experiment"*, Proc. of IEEE Int. Symposium on EMC. August 2003, Boston, USA, pp. 718-723.

[4] F. Arteche and C. Rivetta "*EM Immunity studies for front-end electronics in high-energy physics experiments"*, Proc. of Int. Symposium on EMC, EMC Europe 2004. September 2004, Eindhoven, The Netherlands, pp. 533-538.

[5] IEC - 61000-4-6 *"Electromagnetic compatibility - Testing and measurement techniques – Immunity to conducted disturbances, induced by radio-frequency fields"*. Basic EMC publication, Ed. 2000.

[6] S. Pignari and F. G. Canavero, *"Theoretical assessment of bulk current injection versus radiation"*, IEEE Trans. on EMC. vol. 38, no. 3, pp. 469-477, August 1996.

[7] G. Spadacini and S. A. Pignari, *"A bulk current injection test conforming to statistical properties of radiation-induced effects"*, IEEE Trans. on EMC. vol. 46, no. 3, pp. 446-458, August 2004.

[8] Katja Klein *et. al.* "*The CMS Silicon Strip Tracker - Overview and Status*", HEP2005 International Euro-physics Conference on High Energy Physics, Lisboa, Portugal, July 2005.

[9] M. Beattie and L.T. Pileggi, *"On-chip induction modeling: basics and advanced methods"* IEEE Trans. on Very Large Scale Integration (VLSI) Systems., vol. 10, no. 6, pp. 712-729, Dec. 2002.

[10] A.Ruehli, *"Inductance calculations in Complex Integrated Circuit Environment"*, IBM Journal Research & Development, vol 16, no 5, pp 470-481, September 1972.